AFRL-RV-PS-
TR-2013-0137

HYPERTHERMAL CARBON DIOXIDE INTERACTIONS WITH SELF-ASSEMBLED MONOLAYER SURFACES

Timothy Minton

Montana State University, Inc.
Office of Sponsored Programs
307 Montana Hall
Bozeman, MT 59717-0001

8 September 2013

Final Report

AIR FORCE RESEARCH LABORATORY
Space Vehicles Directorate
3550 Aberdeen Ave SE
AIR FORCE MATERIEL COMMAND
KIRTLAND AIR FORCE BASE, NM 87117-5776

DTIC COPY

NOTICE AND SIGNATURE PAGE

Using Government drawings, specifications, or other data included in this document for any purpose other than Government procurement does not in any way obligate the U.S. Government. The fact that the Government formulated or supplied the drawings, specifications, or other data does not license the holder or any other person or corporation; or convey any rights or permission to manufacture, use, or sell any patented invention that may relate to them.

This report is the result of contracted fundamental research deemed exempt from public affairs security and policy review in accordance with SAF/AQR memorandum dated 10 Dec 08 and AFRL/CA policy clarification memorandum dated 16 Jan 09. This report is available to the general public, including foreign nationals. Copies may be obtained from the Defense Technical Information Center (DTIC) (http://www.dtic.mil).

AFRL-RV-PS-TR-2013-0137 HAS BEEN REVIEWED AND IS APPROVED FOR PUBLICATION IN ACCORDANCE WITH ASSIGNED DISTRIBUTION STATEMENT.

//SIGNED//	//SIGNED//
Dr. Benjamin Prince, AFRL/RVBXT Program Manager	Edward J. Masterson, Colonel, USAF Chief, Battlespace Environment Division

This report is published in the interest of scientific and technical information exchange, and its publication does not constitute the Government's approval or disapproval of its ideas or findings.

Approved for Public Release; distribution is unlimited.

REPORT DOCUMENTATION PAGE

Form Approved
OMB No. 0704-0188

1. REPORT DATE *(DD-MM-YYYY)*	2. REPORT TYPE	3. DATES COVERED *(From - To)*
08-09-2013	Final Report	19 Jan 2011 to 19 Apr 2013

4. TITLE AND SUBTITLE
Hyperthermal Carbon Dioxide Interactions with Self-Assembled Monolayer Surfaces

5a. CONTRACT NUMBER
FA9453-11-1-0223

5b. GRANT NUMBER

5c. PROGRAM ELEMENT NUMBER
62601F

6. AUTHOR(S)
Timothy Minton

5d. PROJECT NUMBER
1010

5e. TASK NUMBER
PPM00010071

5f. WORK UNIT NUMBER
EF004020

7. PERFORMING ORGANIZATION NAME(S) AND ADDRESS(ES)
Montana State University, Inc.
Office of Sponsored Programs
307 Montana Hall
Bozeman, MT 59717-0001

8. PERFORMING ORGANIZATION REPORT NUMBER

9. SPONSORING / MONITORING AGENCY NAME(S) AND ADDRESS(ES)

Air Force Research Laboratory
Space Vehicles Directorate
3550 Aberdeen Avenue SE
Kirtland AFB, NM 87117-5776

10. SPONSOR/MONITOR'S ACRONYM(S)
AFRL/RVBXT

11. SPONSOR/MONITOR'S REPORT NUMBER(S)
AFRL-RV-PS-TR-2013-0137

12. DISTRIBUTION / AVAILABILITY STATEMENT
Approved for Public Release; distribution is unlimited.

13. SUPPLEMENTARY NOTES

14. ABSTRACT

We have conducted new investigations of the energy transfer dynamics of CO_2 scattering from fluorocarbon liquid and self-assembled monolayer (SAM) surfaces, using the direct comparison of the scattering behavior from the liquid and semi-solid surfaces to allow new insight into the pivotal initial step in gas-surface reaction dynamics. Specific interests are to probe the influence of surface structure vs. mass effects on the scattering dynamics and the role of the structure of the incident projectile. Molecular beams of CO_2 were directed onto the surfaces, and velocity and angular distributions of inelastically scattered species were determined from time-of-flight distributions collected for various initial and final angles with the use of a rotatable mass spectrometer. All velocity distributions were bimodal and were interpreted in terms of two limiting cases of direct inelastic scattering (IS) and thermal desorption (TD). The average final velocity of the IS component depended on the deflection angle ($\chi = 180° - (\theta_i + \theta_f)$), and the IS velocity distribution could not be described in terms of a temperature. The more specular angular distributions for the IS products from the SAM surfaces suggest that the SAM surfaces are smoother than the liquid surfaces. Still, there is more energy transfer on the SAM surfaces, which is likely the result of significant deflection of SAM chains during the collision in comparison with molecular fragments on the liquid surfaces. We have demonstrated that a simple kinematic analysis that models the scattering as an incident sphere interacting with a sphere-like localized region of the surface with a finite effective mass describes the energy transfer well even though the incident species is a molecule with internal structure. The success of the simple kinematic model in explaining energy transfer data for molecular projectiles suggests that this model may be of general use in describing collisions of gas-phase species with liquid and semi-solid surfaces.

15. SUBJECT TERMS
Surface Interactions, Hyperthermal Carbon Dioxide, Self-Assembled Monolayers, Energy Transfer, Molecule-Surface Collisions

16. SECURITY CLASSIFICATION OF:			17. LIMITATION OF ABSTRACT	18. NUMBER OF PAGES	19a. NAME OF RESPONSIBLE PERSON
a. REPORT	b. ABSTRACT	c. THIS PAGE			Dr. Benjamin Prince
Unclassified	Unclassified	Unclassified	Unlimited	24	19b. TELEPHONE NUMBER *(include area code)*

This page is intentionally left blank.

Table of Contents

List of Figures

1. INTRODUCTION

The Air Force Research Laboratory's Space Vehicles Directorate has been developing a sensor that can be used on miniature satellites to detect the flux of low-energy atoms at low-Earth orbital (LEO) altitudes, in order to enable accurate 3-D specification of the magnetosphere in real time as well as density measurements of the thermosphere. The sensor under current development is based on the charge conversion of hyperthermal oxygen atoms (O) to their anionic form (O^-) upon collision with an organosilane/silicon self-assembled monolayer (SAM). The measured current of O^- can be related to the flux of O atoms striking the sensor surface. Enhancements of as much as a factor of 2 in the ion yield have been seen on SAM surfaces as compared with a standard polished tungsten surface, suggesting that the electronic properties of nanostructures can enhance anion formation in hyperthermal atom-surface scattering events. Because the hyperthermal O-atom source at AFRL produces a low flux at low kinetic energies near 5 eV, the experiments have difficulty probing the efficacy of charge exchange in this most relevant energy regime. Furthermore, the lifetime of these SAM-based sensors has not been assessed. Reactions of hyperthermal oxygen atoms might erode the organic material on the surfaces and reduce their efficiency at charge conversion.

The original goals of this project were to (1) measure the lifetimes of AFRL-provided SAMs under hyperthermal O-atom bombardment, (2) study the dynamics of O-atom interactions with the SAM surfaces, and (3) investigate the utility of an alternative solid-state sensor approach from the UK. These goals have not been realized. The move of the AFRL from Hanscom to Kirtland and the accompanying loss of the AFRL points of contact who were knowledgeable about this project led to a delay of more than a year in the ability of AFRL staff to deliver the SAM samples. By the time the capability of the AFRL to deliver the SAM samples was restored, the PI's apparatus had become disabled by a serious problem with the mass spectrometer detector, which required about one year to repair and then several months of testing to re-optimize its performance. Furthermore, while the apparatus was operational, the PI contacted the UK group who had made atomic-oxygen sensors in the past, but this group had decided to abandon this area of research and no longer possessed the technical ability or desire to produce solid-state sensors for testing. During the time that the PI's lab was waiting for the AFRL to be moved and set up again at Kirtland, a related study was undertaken in the PI's lab to probe the scattering dynamics of atoms and molecules on liquid and SAM surfaces, in order to deepen the understanding of gas-surface interactions at liquid and semi-solid surfaces and to train personnel in the PI's lab for studies of gas-surface interaction dynamics. This effort, which was funded by the project, has proven to be fruitful and the results of these studies are the subject of this report.

2. BACKGROUND

The interfacial region in a gas-surface collision provides the initial environment for reaction and, possibly, solvation. The scattering mechanisms of a gaseous atom or molecule from a liquid or (more ordered) SAM surface depend on the chemical and physical nature of the surface. Translational, rotational, and vibrational energy transfer dynamics play a role in controlling the

interaction of incident atoms or molecules on the surface and the ejection of these species back into the gas-phase.[1-4]

Previous studies of atom and molecule scattering at the gas-liquid and gas-SAM interface have developed a basic picture of the gas-surface collision dynamics. The previous experiments showed a bimodal distribution for the scattered products, in which they exited the surface with two qualitatively different types of trajectories: impulsive scattering (IS) and thermal desorption (TD). Impulsively scattered species transfer a fraction of their energy to the surface during collisions and scatter back into the vacuum with a reduced translational energy. If the incident species have superthermal velocities, then the IS products are still superthermal, although less so. Thermally desorbed species desorb from the surface with a Maxwell-Boltzmann (M-B) distribution of velocities characteristic of the surface temperature. The angular-dependent flux of the TD species follows a cosine distribution about the surface normal, while the IS species scatter in a lobular angular distribution, peaking at a direction near specular angle. Thus, IS species retain memory of their incidence energy and angle, while TD species do not.

Several groups have conducted detailed studies of the energy transfer at the gas-liquid interface. The Nathanson group has reported the nonreactive scattering dynamics between energetic atoms and liquid surfaces including squalane,[5,6] perfluorinated polyether (PFPE),[7-9] and liquid metals.[10,11] The Minton group has studied the reactive scattering of hyperthermal oxygen atoms scattering from squalane and ionic liquids.[3,12] Nathanson, Minton, and co-workers have also observed a deflection rule from the scattering experiments of rare-gas atoms from squalane and PFPE surfaces,[8,13] indicating a localized collision with a region of the surface with a finite effective mass. Nesbitt and co-workers have conducted detailed studies on the nonreactive interaction between CO_2 molecules and a PFPE liquid surface.[4,14-20] They suggested a two-temperature model, in which both the rotational and translational energy distributions of IS and TD components of the scattered molecules may be described by a temperature. The conclusion that the translational energy distributions of the IS molecules may be described by a temperature is at odds with the results of the research which is presented below.

Gas-surface collision dynamics studies using SAMs were first performed by Naaman and coworkers to study energy transfer from atoms and molecules to model organic surfaces.[21,22] SAMs were used because they form ordered organic surfaces with specific structure and they have functional groups of interest located at the gas-surface boundary. Recent experimental and theoretical studies of gas-surface interactions with SAM surfaces have been performed by Hase, Morris, Troya, and coworkers.[23-30] Fluorocarbon SAMs (F-SAMs) have been used in simulations as a comparison to the experimental results of CO_2 molecules scattered from PFPE surfaces because SAM surfaces serve as more theoretically tractable surfaces that are presumed to resemble the liquid surfaces.[20,26,31,32]

Here, we provide complementary information to the previously determined rotational distributions by measuring translational energy and angular distributions of scattered CO_2 molecules from PFPE and F-SAM surfaces with very high resolution. In the experiments, CO_2 molecules with initial translational energies of 10.6 and 4.7 kcal mol^{-1} were directed at 300 K surfaces, and the scattered products were detected by a mass spectrometer.

3. METHODS, ASSUMPTIONS, AND PROCEDURES

The experiments were performed using a crossed molecular beams apparatus with a rotatable mass spectrometer and a supersonic beam source (see Fig. 1).[3,8,33] A continuous supersonic beam containing carbon dioxide molecules was directed at a sample surface and the scattered products were collected by the rotatable mass spectrometer. The PFPE was held in a liquid reservoir; the F-SAM sample was mounted by clamping in it between two copper plates with a 1 cm × 1 cm square front window. Liquid and SAM surfaces were prepared such that the surface normal and the detector rotation axis were in the same plane, and this axis passed through the sample surface. Number density distributions as a function of arrival time at the detector (known as "time-of-flight," or "TOF" distributions) of the scattered molecules were measured as a function of incidence angle (θ_i) and final angle (θ_f), with respect to surface normal. Each TOF distribution was initiated when one of the 1.5 mm slots of a spinning slotted disk ("chopper wheel," 150 Hz) passed in front of the opening to the detector. The flight path from the chopper wheel to the ionizer of the mass spectrometer detector was 29.4 cm. To obtain the velocity distribution of the incident beam, the samples were lowered out of the beam path and TOF distributions of the beam were collected with the detector aligned along the beam axis. The average translational energies of the two beams used were 10.6 kcal mol^{-1} and 4.7 kcal mol^{-1}. The 10.6 kcal mol^{-1} carbon dioxide molecular beam was generated by expanding a 1000 Torr mixture of 9.65% CO_2 in H_2 through a 50 μm nozzle heated to 70 °C. The 4.7 kcal mol^{-1} beam was generated by expanding a 1000 Torr mixture of 25% CO_2 in He with a nozzle temperature of 50 °C. Translational energy distributions were derived from the TOF distributions by straightforward methods, and average translational energies were then calculated.[34] The incidence angles were 30°, 45°, and 60°. The final angles (θ_f) started from 35°, 20°, and 5°, respectively, and increased in 5° increments up to 70°.

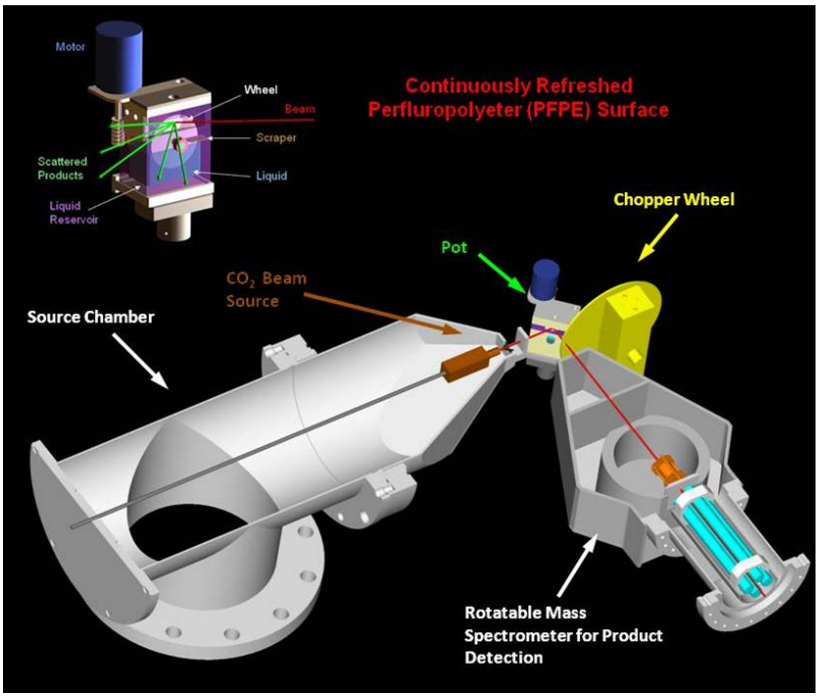

Figure 1. Schematic diagram of the experimental apparatus.

The PFPE thin film was produced by using the method of Lednovich and Fenn.[35] First, 37 mL of Krytox 1618[36] was degassed under a rough vacuum for more than 12 hours before putting it in a liquid reservoir in the vacuum chamber. A continuously refreshed PFPE film was generated by rotating a polished stainless-steel wheel through the liquid reservoir which was held at 300 K. The 0.25 Hz rotating wheel dragged a thick film of PFPE upwards and was cleaned by a sapphire scraper which left a 100-μm-thick film on the rotating wheel.[37] The F-SAM sample was provided by the Morris group from Virginia Tech. It was prepared by spontaneous chemisorption of alkanethiols on gold wafers using 1 mM ethanolic solutions of (1H, 1H, 2H, 2H)-perfluoro-decanethiol.[23]

4. RESULTS

Representative TOF distributions of CO_2 molecules scattered from both PFPE and F-SAM surfaces are shown in the left panels of Fig. 2. These TOF spectra were collected at a final angle of 60° following impingement by CO_2 molecules at an incidence angle of 60° with average translational energies of 10.6 kcal mol^{-1} and 4.7 kcal mol^{-1}. As in our previous studies, the analysis of the TOF distributions assumed that the molecules scattered in two distinct distributions, with IS products arriving at shorter times and TD arriving at longer times.[3,7,12,34] The TD components were assumed to correspond to CO_2 molecules that scatter with a MB distribution of final translational energies corresponding to the surface temperature:

$$I_{TD} \propto \frac{E_f}{(RT_S)^2} e^{-E_f/RT_S} \qquad (1)$$

The TD molecules lose memory of their initial translational energies and angles, E_i and θ_i, after reaching thermal equilibrium with surface.[1] These molecules desorb from the surface in a cosine flux distribution with respect to surface normal. In order to separate the IS and TD components, the TOF distribution of the TD products is calculated using the assumption of a M-B distribution and the appropriate density-to-flux conversion.[34] The difference between the overall TOF distribution and the assumed TD component is taken to be the IS component of scattered molecules, which corresponds to the molecules that scattered from the surface before thermal equilibrium was established. The translational energy distributions of the IS molecules were then obtained from the IS components of the TOF distributions. The corresponding translational energy distributions are shown in the right panels of Fig. 2. As the translational energy distributions are proportional to flux, the relative fluxes of TD and IS components can be obtained by integrating the components of the translational energy distributions. Average final energies may also be obtained from the translational energy distributions.

It was suggested by Nesbitt and co-workers that the translational distributions of the IS CO_2 molecules have a temperature that is equivalent to the rotational temperature of the molecules.[4, 14-20] This conclusion was based on experiments in which the rotational energy distributions of the scattered CO_2 molecules were measured. They measured two populations of rotational distributions, one corresponding to the surface temperature and the other corresponding to a much higher temperature. They suggested that the rotational and translational energies of the IS

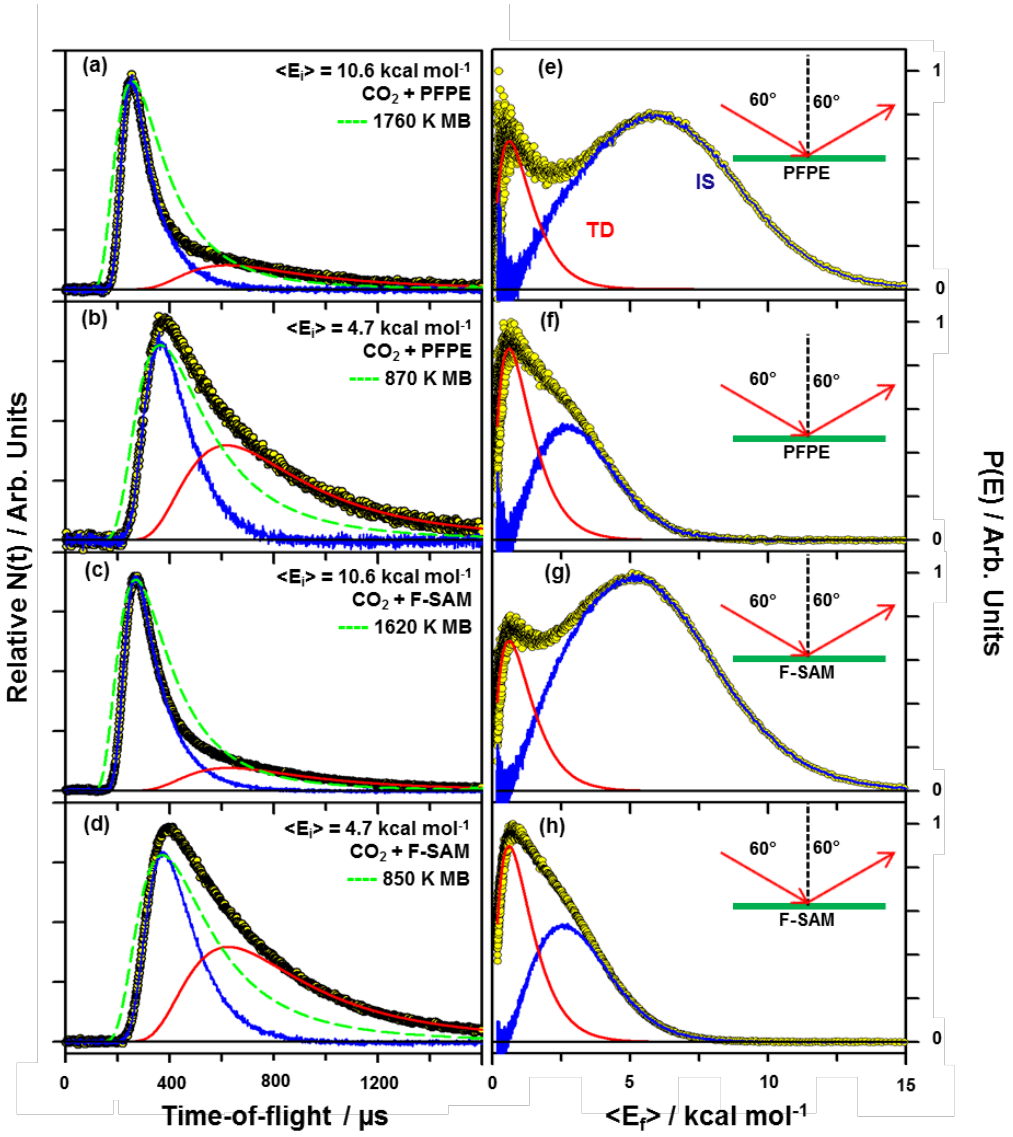

Figure 2. Representative TOF and translational energy distributions.

molecules should be the same, and they had lower-resolution translational energy data to support this supposition. We tried to find M-B distributions that would give good fits to our IS TOF data (see the green dashed curves in Fig. 2), but it was clear that the measured TOF distributions were much too narrow to be described by M-B distributions and that the IS molecules definitely did not have a translational energy distributions that could be described in terms of a temperature.

The flux angular distributions of the CO_2 molecules that scattered from the PFPE and F-SAM surfaces with $\theta_i = 60°$ are shown in Fig. 3. The TD flux follows a cosine distribution with respect to the surface normal, while the IS flux exhibits lobular scattering in the forward (specular) direction. An interesting observation is the narrower angular scattering distribution of the IS molecules from the F-SAM surface than from the PFPE surface, suggesting that the SAM surface is smoother than the PFPE surface.

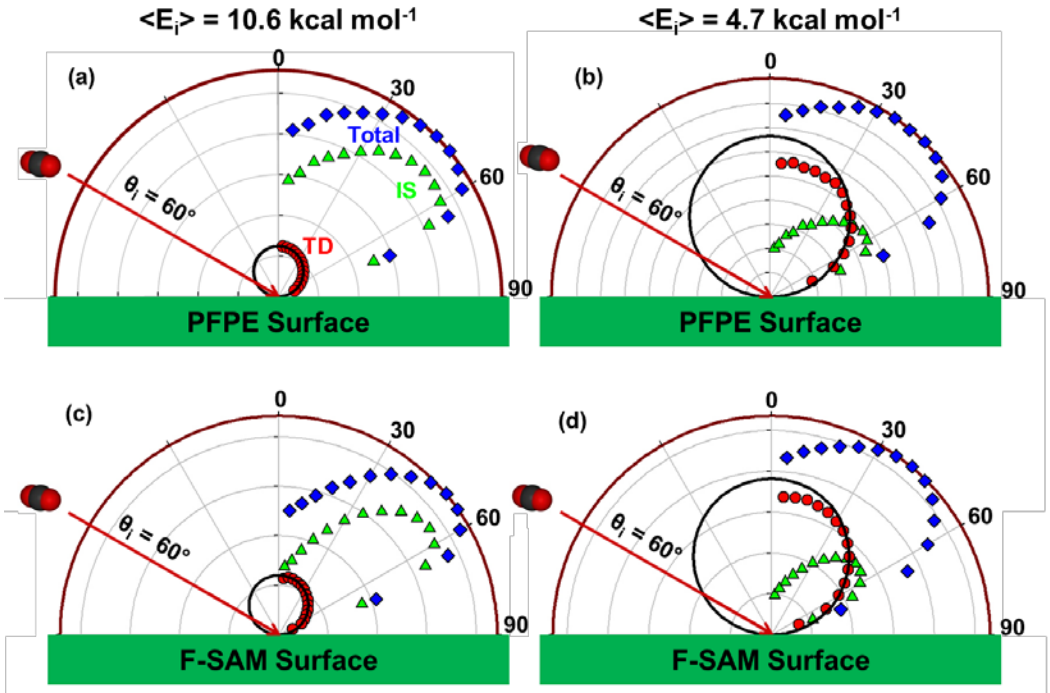

Figure 3. Angular distributions of scattered CO_2 flux.

The fraction of molecules that may be described as TD is plotted as a function of final angle for CO_2 molecules with $\langle E_i \rangle$ = 10.6 kcal mol^{-1} scattering from a PFPE surface in Fig. 4. For a fixed incidence angle, the TD fraction decreases with θ_f. This trend is most obvious with $\theta_i = 60°$ because of the fact that impulsive scattering is more favored for higher incidence angles. For CO_2 molecules that scattered with $\langle E_i \rangle$ = 4.7 kcal mol^{-1}, the TD components do not follow perfect cosine distributions (Fig. 3). This result reflects the difficulty of separating IS and TD components when the incidence energy is low, because the two components overlap strongly. In fact, when the incidence energy is low, the concept of two distinct types of scattering breaks down, as even the IS molecules tend to exit the surface with near-thermal velocities. This is more obvious for smaller final angles where thermal scattering is at its largest.

The average energies of the IS CO_2 molecules as a function of final angle at each incidence angle were calculated. The energy lost from translation for the scattered CO_2 molecules, which is defined as the difference of incidence and final translational energies divided by the incidence energy, was plotted as a function of deflection angle ($\chi = 180° - (\theta_i + \theta_f)$) in Figure 5.[8] From the graphs, it could be concluded that the energy transfer increases with the angle of deflection. This suggests that the collision dynamics follow a deflection rule, which says that the energy transferred during collisions does not depend on either the incidence angle or the final angle alone, but that energy transfer only depends on the deflection angle.

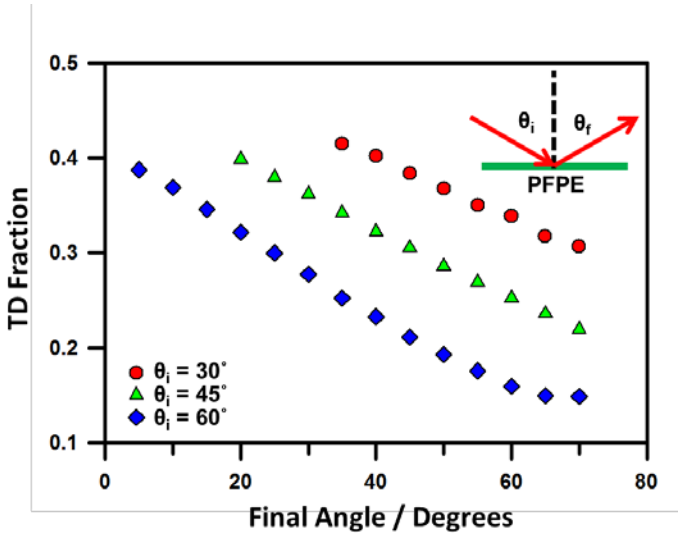

Figure 4. Fraction of thermally desorbed CO_2 as a function of final angle.

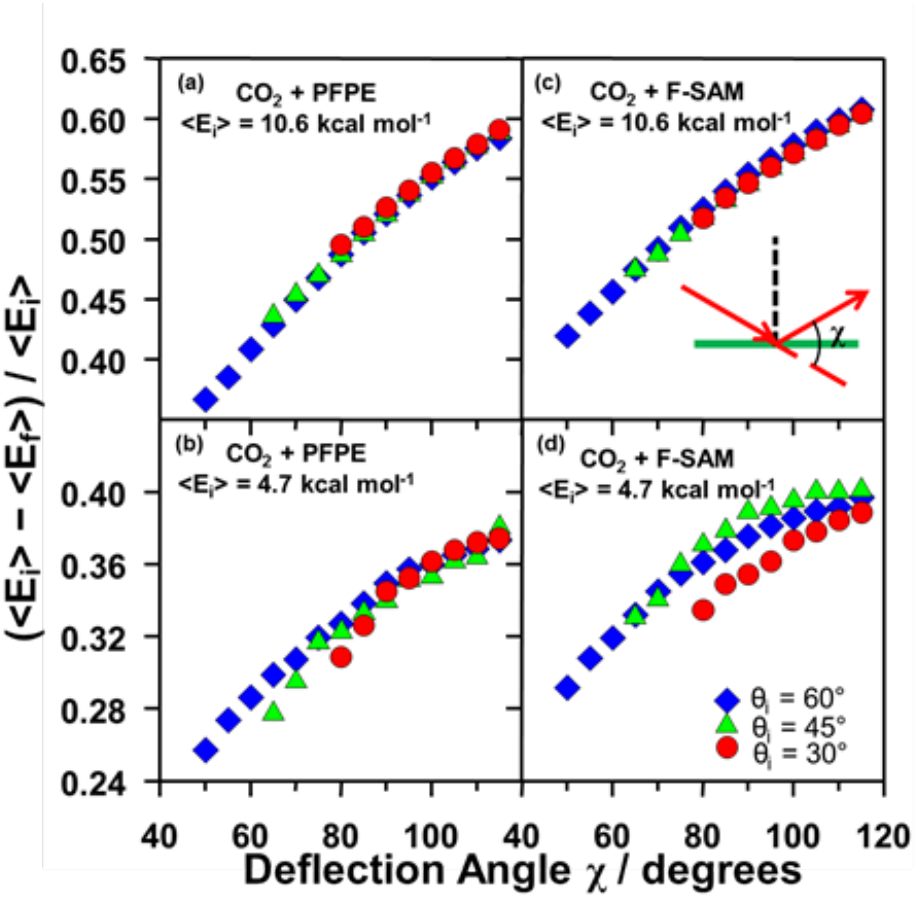

Figure 5. Fractional energy transfer as a function of deflection angle.

5. DISCUSSION

The TOF and translational energy distributions of scattered CO_2 molecules are bimodal and appear similar for scattering on both PFPE and F-SAM surfaces. The components with shorter flight times are impulsive scattering (IS) components with higher translational energies, which correspond to a non-thermal gas-surface interaction. These molecules lose only a fraction of their kinetic energy to internal motion, either on the surface or in the scattered molecule, and are scattered back into the vacuum after one or a small number of collisions. The components with a longer flight times are thermal desorption (TD) components. For molecules to follow the TD pathway, essentially all of their incidence translational energy is lost during the collision. They desorb into the vacuum with a M-B distribution of velocities at the surface temperature. The flux of TD components has a cosine distribution with respect to surface normal, while the flux of IS components exhibits a lobular distribution peaked near the specular direction.

Changing the incidence energy affects the weights of the TD and IS components. As shown in Fig. 2, the fraction of TD scattering increased from 15.9% to 43.2% between panels (e) and (f) where the incidence energy of CO_2 molecules on the PFPE surface decreased from 10.6 kcal mol^{-1} to 4.7 kcal mol^{-1}. The fraction of TD scattering changed similarly from 14.2 % to 43.1% between panels (g) and (h) in Fig. 2, for scattering on the F-SAM surface. Flux angular distributions plotted in Fig. 3 also show the increase in TD scattering with a decrease in incidence energy. This suggests a stronger or longer gas-surface interaction at lower incidence energies. The change in incidence energy also affects the energetics of the scattered products. The fraction of energy transferred into internal motion for the IS component decreased from 40.9% to 28.6% between panels (e) and (f) and from 45.7% to 31.9% between panels (g) and (h) in Fig. 2. The transfer of larger amounts of energy to internal motion at higher incidence energies indicates that the surfaces are far from being rigid during the collision events.

Figure 4 shows that the fraction of CO_2 molecules that follow the TD pathway after impinging on the PFPE surface decreases with an increase in final angle, while holding the incidence angle constant. Scattered products from both PFPE and F-SAM surfaces with both incidence energies share the same trend. When holding the incidence angle constant, the TD fraction decreases with an increase in final angle (shown in both Fig. 3 and Fig. 4). This could be the result of an increase in multiple-bounce interactions that drive the molecules into thermal equilibrium with the surface when the molecules strike more normal to the surface.

The energy transfer of the IS CO_2 molecules follows the deflection rule observed in the inelastic scattering studies of rare gas atoms on PFPE and squalane by Nathanson and Minton.[8] Such scattering behavior suggests that energy transfer is only dependent on the deflection angle rather than incidence or final angle individually. Recently, Minton and Nathanson have used a "soft-sphere" scattering model to describe atom scattering on liquid and SAM surfaces under conditions where the deflection rule appears to hold.[38] This model pictures the incoming atoms as spheres that interact with a localized spherical region of the surface with an effective mass. Figure 6 shows the result of applying this model to the fractional energy transfer data for CO_2 molecules scattering impulsively from PFPE and F-SAM surfaces with $\langle E_i \rangle$ = 10.6 kcal mol^{-1}. The model describes the data almost perfectly and yields effective surface masses of 264 and 319 amu for the PFPE and F-SAM surfaces, respectively. The lower effective surface mass

for the F-SAM surface is attributed to the lower density of this surface, which is more "floppy" and has more lower-frequency vibrational modes, allowing more surface atoms to become involved in the collision. This is the first application of the soft-sphere model to the scattering of molecules, which have internal structure, as opposed to atoms. Even though the CO_2 molecules have a non-spherical structure and can themselves absorb energy in the collision (becoming rotationally excited), the transfer of translational energy to internal degrees of freedom can still be described by a sphere-like scattering model. This result is remarkable and suggests the soft-sphere picture of gas-surface scattering is robust even for molecules.

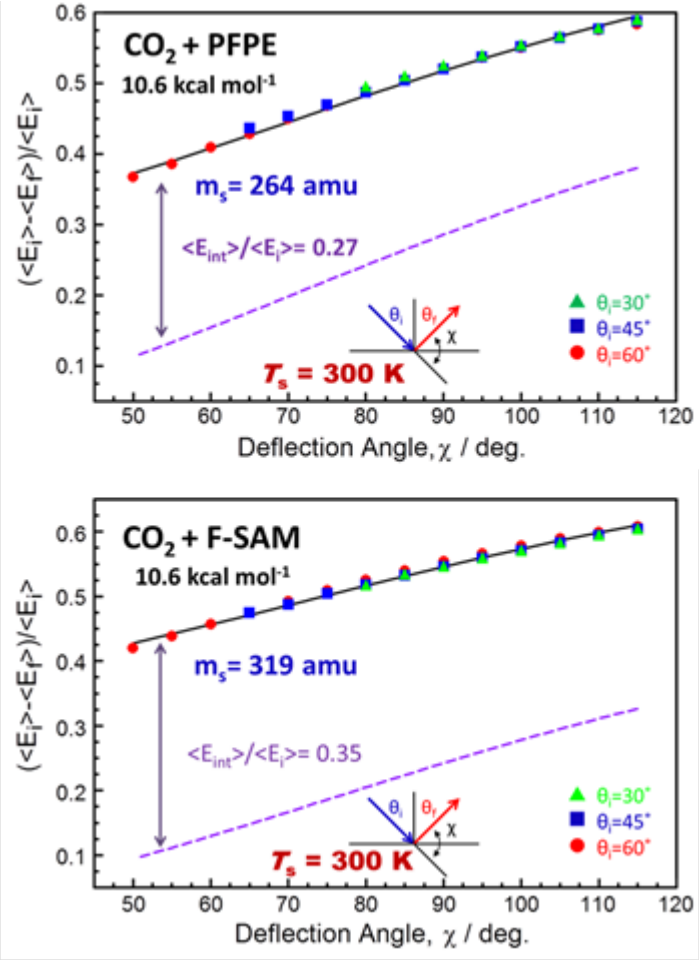

Figure 6. Fit of kinematic soft-sphere model to fractional energy transfer data.

The dynamical behaviors of CO_2 molecules scattered from both PFPE and F-SAM surfaces have been directly compared, in order to observe the differences between these two surfaces. For fixed θ_i and $\langle E_i \rangle$, the angular flux distribution of the IS component is more specular (IS intensity decreases faster when moving away from the specular direction) for scattered molecules from the F-SAM surface than from the PFPE surface. This indicates that the surface of PFPE is rougher than the surface of F-SAM. Although the rougher surface of the PFPE might lead one to conclude that energy transfer should be larger on the PFPE surface, the energy transfer is more

efficient for collisions of CO_2 molecules on F-SAM surface. This is likely the result of the lower density of the F-SAM surface, which, as mentioned above, also leads to a higher effective surface mass. Hase and co-workers have done simulations of Ne scattering from SAM surface in order to study the energy transfer efficiency and have pointed out the possibility for energy transfer between the SAM chains.[30]

In their work on CO_2 molecules scattering from PFPE surfaces, Nesbitt and co-workers presented a two temperature (or "two-Boltzmann") model for the translational energy distribution of the scattered products. This model suggests that the translational energy distribution of the scattered products may be separated into two components, each following a M-B distribution. The lower temperature is close to the surface temperature and therefore corresponds to the TD component, while the higher temperature is far from the surface temperature and corresponds to the IS component. For the data presented in Fig. 2, we attempted to fit the peaks of the IS components to M-B distributions with temperatures higher than the surface temperature. The IS component was then subtracted from the total TOF distribution to yield the TD component, but it was too narrow to be fitted into a Boltzmann distribution. We have also tried to fit the total TOF distribution with two M-B distributions without separating IS and TD components. This fit sets one temperature equal to the temperature of the surface and finds the best fit for the higher temperature and the coefficients for both M-B distributions. No matter what we tried, it was impossible to fit the TOF distributions with two M-B distributions. We must therefore conclude that the translational energy distributions of impulsively scattered CO_2 molecules cannot be described by a temperature, in contradiction to the conclusion of Nesbitt and coworkers.

Simulations of CO_2 molecules scattered from the F-SAM surface have been performed by Hase and co-workers to study the translational energy ($P(E_f)$) and rotational angular momentum (P(J)) distributions.[31] It has been found that these two distributions are different at all collisions for direct trajectories, due to the complexity of the dynamics. Based on their studies, P(J) for the IS products could be described in terms of a temperature that is significantly higher than the temperature of the surface, while the P(E) could only been described as a high-energy non-Boltzmann component. This finding is in agreement with the experimental results presented here, as well as the Boltzmann rotational energy distributions reported by Nesbitt and coworkers.

6. CONCLUSIONS

The gas-surface scattering dynamics of CO_2 molecules on perfluorinated polyether (PFPE) and perfluorinated self-assembled monolayer (F-SAM) surfaces were investigated by directing a supersonic molecular beam of CO_2 at a continuously refreshed liquid PFPE surface and a static F-SAM surface and collecting time-of-flight and angular distributions of the inelastically scattered CO_2 molecules, with the use of a rotatable mass spectrometer detector. The CO_2 molecules collided with the surfaces (held at 300 K) with incidence energies of either 10.6 kcal mol^{-1} or 4.7 kcal mol^{-1}. Incidence angles were 30°, 45°, and 60° with respect to surface normal. The scattered products could be divided into two components, impulsive scattering (IS) and thermal desorption (TD). For the IS component, CO_2 molecules scattered from the surface mainly in the specular direction while maintaining a large fraction of their initial translational energy. The average fractional energy transfer of the impulsively scattered molecules was

dependent on the deflection angle ($\chi = 180° - (\theta_i + \theta_f)$), and the energy transfer data for IS CO_2 molecules could be described well by a kinematic model which assumes that the incoming CO_2 molecule interacts with a localized region of the surface with an effective mass in a gas-phase-like collision. For the TD component, CO_2 molecules exited the surface in a cosine distribution about the surface normal, with a Maxwell-Boltzmann (M-B) distribution of velocities given by the surface temperature. Scattering dynamics on these fluorinated liquid and SAM surfaces were compared directly. It was found that the scattering dynamics were very similar, but with differences: First, the more specular behavior of the IS products from the F-SAM surface indicated that its surface was smoother than that of the PFPE. Second, although the smaller roughness might lead one to assume that energy transfer would be less on the F-SAM surface, it was actually larger. The increased energy transfer on the F-SAM surface may be the result of its lower density and consequent lower frequency surface modes, which are easier to excite during a collision with a CO_2 molecule.

REFERENCES

[1] Nathanson, G. M., Molecular beam studies of gas-liquid interfaces, *Ann. Rev. Phys. Chem.,* **2004,** *55*, pp. 231-255.

[2] Minton, T. K., M. Tagawa, and G. M. Nathanson, Energy Accommodation in Hyperthermal Gas-Surface Collisions: Relevance to Aerobraking in Planetary Atmospheres, *J. Spacecr. Rockets,* **2004,** 41, pp. 389-396.

[3] Zhang, J. M., D. J. Garton, and T. K. Minton, Reactive and inelastic scattering dynamics of hyperthermal oxygen atoms on a saturated hydrocarbon surface, *J. Chem. Phys.,* **2002,** *117*, pp. 6239-6251. Zhang, J. M., H. P. Upadhyaya, A. L. Brunsvold, and T. K. Minton, Hyperthermal reactions of O and O_2 with a hydrocarbon surface: Direct C-C bond breakage by O and H-atom abstraction by O_2, *J. Phys. Chem. B,* **2006**, 110, pp. 12,500-12,511.

[4] Perkins, B. G., T. Haber, and D. J. Nesbitt, Quantum state-resolved energy transfer dynamics at gas-liquid interfaces: IR laser studies of CO_2 scattering from perfluorinated liquids, *J. Phys. Chem. B,* **2005**, 109, pp. 16396-16405.

[5] Saecker, M. E. and G. M. Nathanson, Collisions of Protic and Aprotic Gases with Hydrogen-Bonded and Hydrocarbon Liquids, *J. Chem. Phys.,* **1993**, 99, pp. 7056-7075.

[6] Saecker, M. E., S. T. Govoni, D. V. Kowalski, M. E. King, and G. M. Nathanson, Molecular-Beam Scattering from Liquid Surfaces, *Science,* **1991**, 252, pp. 1421-1424.

[7] Saecker, M. E. and G. M. Nathanson, Collisions of Protic and Aprotic Gases with a Perfluorinated Liquid. *J. Chem. Phys.,* **1994**, 100, pp. 3999-4005.

[8] King, M. E., G. M. Nathanson, M. A. Hanning-Lee, and T. K. Minton, Probing the Microscopic Corrugation of Liquid Surfaces with Gas-Liquid Collisions, *Phys. Rev. Lett.* **1993**, 70, pp. 1026-1029.

[9] King, M. E., M. E. Saecker, and G. M. Nathanson, The Thermal Roughening of Liquid Surfaces and Its Effect on Gas-Liquid Collisions, *Abstracts of Papers of the American Chemical Society,* **1994**, 207, 205-PHYS.

[10] Chase, D. M. Manning, J. A. Morgan, JG. M. Nathanson, and R. B. Gerber, Argon scattering from liquid indium: Simulations with embedded atom potentials and experiment, *J. Chem. Phys.,* **2000**, 113, pp. 9279-9287.

[11] Manning, M., J. A. Morgan, D. J. Castro, and G. M. Nathanson, Examination of liquid metal surfaces through angular and energy measurements of inert gas collisions with liquid Ga, In, and Bi, *J. Chem. Phys.,* **2003**, 119, pp. 12593-12604.

[12] Wu, B. H., J. M. Zhang, T. K. Minton, K. G. McKendrick, J. M. Slattery, S. Yockel, and G. C. Schatz, Scattering Dynamics of Hyperthermal Oxygen Atoms on Ionic Liquid Surfaces: [emim][NTf_2] and [C_{12}mim][NTf_2], *J. Phys. Chem. C,* **2010**, 114, pp. 4015-4027.

[13] King, M. E. K. M. Fiehrer, G. M. Nathanson, and T. K. Minton, Effects of thermal roughening on the angular distributions of trapping and scattering in gas-liquid collisions, *J. Phys. Chem. A,* **1997**, 101, pp. 6556-6561.

[14] Perkins, B. G. and D. J. Nesbitt, High resolution Dopplerimetry of correlated angular and quantum state-resolved CO_2 scattering dynamics at the gas-liquid interface, *Phys. Chem. Chem. Phys.,* **2010**, 12, pp. 14294-14308.

[15] Perkins, B. G. and D. J. Nesbitt, Stereodynamics at the Gas-Liquid Interface: Orientation and Alignment of CO_2 Scattered from Perfluorinated Liquid Surfaces, *J. Phys. Chem. A,* **2010**, 114, pp. 1398-1410.

[16] Perkins, B. G. and D. J. Nesbitt, Quantum-state-resolved CO_2 scattering dynamics at the gas-liquid interface: Incident collision energy and liquid dependence, *J. Phys. Chem. B,* **2006**, 110, pp. 17126-17137.

[17] Perkins, B. G. and D. J. Nesbitt, Quantum-state-resolved CO_2 scattering dynamics at the gas-liquid interface: Dependence on incident angle, *J. Phys. Chem. A,* **2007**, 111, pp. 7420-7430.

[18] Perkins, B. G. and D. J. Nesbitt, Quantum state-resolved CO_2 collisions at the gas-liquid interface: Surface temperature-dependent scattering dynamics, *J. Phys. Chem. B,* **2008**, 112, pp. 507-519.

[19] Perkins, B. G. and D. J. Nesbitt, Correlated angular and quantum state-resolved CO_2 scattering dynamics at the gas-liquid interface, *J. Phys. Chem. A,* **2008**, 112, pp. 9324-9335.

[20] Perkins, B. G. and D. J. Nesbitt, Toward Three-Dimensional Quantum State-Resolved Collision Dynamics at the Gas-Liquid Interface: Theoretical Investigation of Incident Angle, *J. Phys. Chem. A,* **2009**, 113, pp. 4613-4625.

[21] Cohen, S. R., R. Naaman, and J. Sagiv, Translational energy transfer from molecules and atoms to adsorbed organic monolayers of long-chain amphiphiles, *Phys. Rev. Lett.,* **1987**, 58, pp. 1208-1211.

[22] Cohen, S. R., R. Naaman, and J. Sagiv, Rotational and state-resolved translational distributions of NO scattered from organized amphiphilic monolayers, *J. Chem. Phys.,* **1988**, 88, pp. 2757-2763.

[23] Lu, J. W., W. A. Alexander, and J. R. Morris, Gas-surface energy exchange and thermal accommodation of CO_2 and Ar in collisions with methyl, hydroxyl, and perfluorinated self-assembled monolayers, *Phys. Chem. Chem. Phys.,* **2010**, 12, pp. 12533-12543.

[24] Alexander, W. A., J. R. Morris, and D. Troya, Theoretical study of the stereodynamics of CO collisions with CH_3- and CF_3-terminated alkanethiolate self-assembled monolayers, *J. Phys. Chem. A,* **2009**, 113, pp. 4155-4167.

[25] Alexander, W. A., J. R. Morris, and D. Troya, Experimental and theoretical study of CO collisions with CH_3- and CF_3-terminated self-assembled monolayers, *J. Chem. Phys.,* **2009**, 130, p. 15.

[26] Vazquez, S. A., J. R. Morris, A. Rahaman, O. A. Mazyar, G. Vayner, S. V. Addepalli, W. L. Hase, and E. Martinez-Nunez, Inelastic scattering dynamics of Ar from a perfluorinated self-assembled monolayer surface, *J. Phys. Chem. A,* **2007**, 111, pp. 12785-12794.

[27] Day, B. S. and J. R. Morris, Packing density and structure effects on energy-transfer dynamics in argon collisions with organic monolayers, *J. Chem. Phys.*, **2005**, 122, p. 10.

[28] Day, B. S., J. R. Morris, W. A. Alexander, and D. Troya, Theoretical study of the effect of surface density on the dynamics of Ar plus alkanethiolate self-assembled monolayer collisions, *J. Phys. Chem. A,* **2006**, 110, pp. 1319-1326.

[29] Day, B. S., J. R. Morris, and D. Troya, Classical trajectory study of collisions of Ar with alkanethiolate self-assembled monolayers: Potential-energy surface effects on dynamics, *J. Chem. Phys.,* **2005**, 122, p. 12.

[30] Yan, T. Y., N. Isa, K. D. Gibson, S. J. Sibener, and W. L. Hase, Role of surface intramolecular dynamics in the efficiency of energy transfer in Ne atom collisions with a n-hexylthiolate self-assembled monolayer, *J. Phys. Chem. A,* **2003**, 107, pp. 10600-10607.

[31] Martinez-Nunez, E., A. Rahaman, and W. L. Hase, Chemical dynamics Simulations of CO_2 scattering off a fluorinated self-assembled monolayer surface, *J. Phys. Chem. C,* **2007**, 111, pp. 354-364.

[32] Nogueira, J. J., S. A. Vazquez, O. A. Mazyar, W. L. Hase, B. G. Perkins, D. J. Nesbitt, and E. Martinez-Nunez, Dynamics of CO_2 Scattering off a Perfluorinated Self-Assembled Monolayer. Influence of the Incident Collision Energy, Mass Effects, and Use of Different Surface Models, *J. Phys. Chem. A,* **2009**, 113, pp. 3850-3865.

[33] Lee, Y. T., J. D. McDonald, P. R. LeBreton, and D. R. Herschbach, Molecular beam reactive scattering apparatus with electron bombardment detector, *Rev. Sci. Instrum.,* **1969**, 40, pp. 1402-1408.

[34] Minton, T. K., K. P. Giapis, and T. Moore, Inelastic scattering dynamics of hyperthermal fluorine atoms on a fluorinated silicon surface, *J. Phys. Chem. A,* **1997**, 101, pp. 6549-6555.

[35] Lednovich, S. L. and J. B. Fenn, Absolute evaporation rates for some polar and nonpolar liquids, *AICHE J.,* **1977**, 23, pp. 454-459.

[36] Dupont Krytox Vacuum Pump Fluid Product Data Sheets, *Krytox Vacuum Pump Fluid Product Data Sheet,* **2008**.

[37] Nathanson, G. M., P. Davidovits, D. R. Worsnop, and C. E. Kolb, Dynamics and kinetics at the gas-liquid interface, *J. Phys. Chem.,* **1996**, 100, pp. 13007-13020.

[38] Alexander, W. A., J. Zhang, V. J. Murray, G. M. Nathanson, and T. K. Minton, Kinematics and dynamics of atomic-beam scattering on liquid and self-assembled monolayer surfaces, *Faraday Disc.,* **2012**, 157, pp. 355-374.

LIST OF ACRONYMS

AFRL	Air Force Research Laboratory
TOF	time of flight
IS	impulsive scattering
TD	thermal desorption
M-B	Maxwell-Boltzmann
SAM	self-assembled monolayer
F-SAM	Fluorocarbon self-assembled monolayer
PFPE	perfluoropolyether

DISTRIBUTION LIST

DTIC/OCP
8725 John J. Kingman Rd, Suite 0944
Ft Belvoir, VA 22060-6218 1 cy

AFRL/RVIL
Kirtland AFB, NM 87117-5776 2 cys

Official Record Copy
AFRL/RVBXT/Dr. Benjamin Prince 1 cy

This page is intentionally left blank.